

# Gaseous Species as Reaction Tracers in the Solvothermal Synthesis of the Zinc Oxide Terephthalate MOF-5

Steffen Hausdorf, Felix Baitalow, Jürgen Seidel, and Florian O. R. L. Mertens\*

Institut für Physikalische Chemie, TU Bergakademie Freiberg, Leipziger Strasse 29,  
D-09596 Freiberg, Germany

Received: January 31, 2007; In Final Form: March 8, 2007

Gaseous species emitted during the zinc oxide/zinc hydroxide 1,4-benzenedicarboxylate metal organic framework synthesis (MOF-5, MOF-69c) have been used to investigate the reaction scheme that leads to the framework creation. Changes of the gas-phase composition over time indicate that the decomposition of the solvent diethylformamide occurs at least via two competing reaction pathways that can be linked to the reaction's overall water and pH management. From isotope exchange experiments, we deduce that one of the decomposition pathways leads to the removal of water from the reaction mixture, which sets the conditions when the synthesis of an oxide-based (MOF-5) instead of an hydroxide-based MOF (MOF-69c) occurs. A quantitative account of most reactants and byproducts before and after the MOF-5/MOF-69c synthesis is presented. From the investigation of the reaction intermediates and byproducts, we derive a proposal of a basic reaction scheme for the standard synthesis zinc oxide carboxylate MOFs.

## Introduction

The number of known highly porous inorganic–organic hybrid structures has grown exponentially over the past few years. Among the earliest structures described are the zinc oxide carboxylate-based metal organic frameworks discovered by Yaghi and co-workers.<sup>1–3</sup> Although many different metal organic framework (MOF) types have been developed so far, the zinc oxide carboxylate type materials have become somewhat of the paradigm of applied MOF research, and to date, most gas adsorption,<sup>1,4–8</sup> gas separation,<sup>9,10</sup> or catalytic experiments<sup>11–13</sup> were carried out with this class of material; among those most frequently used is zinc oxide (1,4-benzenedicarboxylate, BDC) called MOF-5 and its derivatives. After having changed the original synthesis from a concept where the base for the deprotonation of the carboxylic acid is provided via gas-phase diffusion<sup>13</sup> to one where the base is provided by the solvent itself, the synthesis was significantly simplified and sped up, which led to a large increase in the number of groups working on these materials. Very recently, a microwave-assisted synthesis of MOF-5 material was reported to be completed even within minutes.<sup>14</sup> A large number of zinc oxide carboxylate-based MOFs have been created so far, and semitechnical processes were developed for the preparation and processing of the first MOF-based product.<sup>15</sup> MOFs in general and particularly MOFs with carboxylic acid-based linkers are attractive because they promise the tailoring of special materials, that is, crystal engineering, by simply varying the carboxylic acids or the metal center used.<sup>1,16–18</sup> For carboxylic acids without functional groups, this promise is largely fulfilled, but for linkers that do carry functional groups, there might be an interference of these groups with the intended network creation. Unfortunately, it is just this group of materials that is of highest interest for applications like sensor materials, catalysts, filters, etc. The original intention of this work was to support synthesis

efforts in this direction by creating a better understanding of the general synthesis reaction scheme. Although the synthesis of the zinc oxide carboxylate-based MOFs seems to be conceptually simple, many reports describe reproducibility problems and discrepancies in the resulting structures caused by small parameter changes, some of them hard to identify and quantify.<sup>6,19–22</sup> Among those parameter changes reported were nucleation effects influenced by the reaction vessel material or more exotic ones like vessel shape and fractional volume filling of the vessel.<sup>23</sup> As was indicated by several authors, a critical parameter for the synthesis of MOF-5, which can be seen as a representative of the whole zinc oxide carboxylate MOF class, with zinc nitrate in diethylformamide (DEF) is the initial water content. In some experiments, an attempted MOF-5 synthesis using  $Zn(NO_3)_2 \cdot 6H_2O$  instead of  $Zn(NO_3)_2 \cdot 4H_2O$  led to MOF-69c.<sup>21,24</sup> Rosi et al. demonstrated that MOF-69c can reliably be generated by adding additional water to the MOF-5 recipe.<sup>26</sup> By using partially hydrolyzed DEF, a new structure  $Zn_3\text{-BDC}_4(\text{NH}_2\text{Et}_2)_2$  was found, which incorporates the hydrolysis product  $\text{NH}_2\text{Et}_2^+$ .<sup>25</sup> Greathouse et al. theoretically investigated the influence of water adsorption and estimated that MOF-5 becomes unstable at a water adsorption exceeding 4 mass %.<sup>27</sup> From all of these investigations, an ambivalent role of water can be concluded. On one hand, it will have a negative influence on the  $ZnO$  MOF formation; on the other hand, it is needed for the hydrolysis of the solvent DEF to release base for deprotonating the carboxylic acid.<sup>28</sup> In the work presented here, because of this special role of water, a specific focus was put on the water balance of the reaction.

Although there was a lot of work done in finding new zinc oxide carboxylate MOF structures, there are hardly any reports regarding the basic reaction scheme. Because it is known that the solvent is not inert but acts as a reactant, the basic understanding of its influence is still unclear. Another important part not sufficiently understood is the actual process of slowly deprotonating the carboxylic acids to ensure controlled crystallization. Because, in the presence of nitrate, nitric acid should

\* To whom correspondence should be addressed. E-mail: florian.mertens@chemie.tu-freiberg.de

be formed during the course of the reaction, it is difficult to see how the oxide formation can occur in the presence of such a strong acid even if the decomposition of the solvent releases diethylamine as a base.<sup>29</sup> A feasible mechanism of how to lower the proton activity irreversibly seems to be missing. Because an initial measurement of the pressure build-up during the standard MOF-5 synthesis (recipe, see the Experimental Procedures; headspace, ca. 40% of the solution volume) revealed a pressure rise up to 1 bar, corrected with respect to thermal expansion, the question about the role of gaseous species in the solvothermal synthesis of MOF-5 arose. We found that tracking the gas-phase composition over time is a good method to learn more about the underlying reaction scheme that ultimately leads to the MOF formation. To derive a basic reaction scheme, the gas-phase investigations were supported by the quantitative determination of the content of most intermediates and byproducts in the reaction solution. The measurements were carried out by NMR, ion chromatography, and titration experiments. In contrast to the gas-phase experiments, these experiments were performed after the reactions were completed.

## Experimental Procedures

**General Experiment.** If not otherwise mentioned, the syntheses were carried out in an autoclave (Parr Instrument Co. 4740, 75 mL). Because previous experiments showed an influence of PTFE on the MOF nucleation process, the original PTFE liner was replaced by a glass container. The autoclave was connected via a valve to an evacuated small reservoir (1.8 mL) that allowed us to extract gas samples from the head space of the autoclave. The gas samples were then directly fed into a differentially pumped mass spectrometer (Pfeiffer Vakuum, Omni Star). After closing off the valve to the mass spectrometer, Fourier transform infrared (FTIR) measurements were taken by flushing out the remaining sample gas with argon into the spectrometer (Varian Excalibur 3100, 650–4000 cm<sup>-1</sup>, MCT detector). The mass spectra peak intensity changes due to the sample extraction were corrected according to the pressure losses in the gas-phase. The pressure changes were independently measured by a pressure gauge. To track the temporal development of the gas-phase composition in the MOF experiment, samples of the gas-phase were taken approximately every 60 min and analyzed by quadrupole mass spectrometry (QMS) and FTIR. For the quantitative evaluation of the mass spectra, the cracking patterns of CO<sub>2</sub> and H<sub>2</sub> were separately measured and calibration curves of peak intensities as a function of the partial pressure composition were taken. The reproducibility and the temporal stability of the calibration as well as the lack of any observable signal cross talk permitted a quantitative estimate of the partial pressures of the main components CO<sub>2</sub> and H<sub>2</sub>. The water content of the reaction solution was determined by Karl Fischer titration, nitrate concentrations by ion chromatography (Dionex DX-100), and Zn<sup>2+</sup> concentrations by inductively coupled plasma-optical emission spectroscopy (ICP-OES). <sup>13</sup>C and <sup>1</sup>H NMR (Bruker DPX 400) were used to identify and/or quantify various byproducts. Solutions were prepared for the ion chromatography measurements by diluting the reaction solution by a factor of 1000 with DI water. Solid precipitates were analyzed by X-ray powder diffraction (XRD) (Siemens D5000 using the Cu K $\alpha$  line).

**Synthesis.** In this work, a standard MOF-5 synthesis is defined by the employment of the following protocol. The solvent DEF was dried over CaH<sub>2</sub> for about an hour until no more hydrogen evolution was observed. Zn(NO<sub>3</sub>)<sub>2</sub>·4H<sub>2</sub>O (1.333

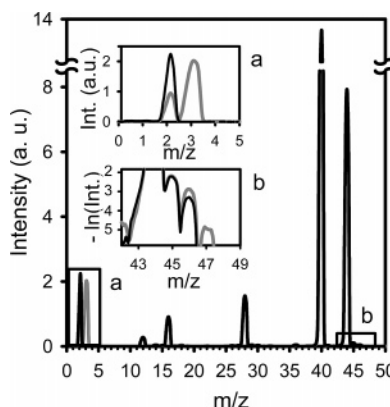


**Figure 1.** Composition of the gas-phase from a MOF-5 synthesis after a reaction time of 24 h. The black line belongs to a standard MOF-5 experiment. The gray line belongs to an experiment using D<sub>2</sub>BDC and Zn(NO<sub>3</sub>)<sub>2</sub>·4D<sub>2</sub>O. Insert a shows the area corresponding to the H<sub>2</sub> and HD species. Insert b shows the area of the masses 45, 46, and 47 corresponding to CO<sub>2</sub> and formic acid, that is, <sup>13</sup>C<sup>16</sup>O<sub>2</sub><sup>+</sup>, <sup>18</sup>O<sup>12</sup>C<sup>16</sup>O<sup>+</sup>, H<sup>12</sup>C<sup>16</sup>O<sub>2</sub>H<sup>+</sup>, and H<sup>12</sup>C<sup>16</sup>O<sub>2</sub>D<sup>+</sup>.

g, 5.1 mmol) (Merck, 98.5%) was dissolved together with H<sub>2</sub>BDC (0.282 g, 1.7 mmol) (Aldrich, 98%) in 16 mL of DEF (ABCR, 99%). Three milliliters of this solution was separated for the analysis of the Zn<sup>2+</sup>, NO<sub>3</sub><sup>-</sup>, and H<sub>2</sub>O content. The solutions were prepared in an argon-filled glove box and only briefly exposed to air during the filling of the autoclave. The autoclave with 13 mL of solution was afterward purged with argon, heated, and kept at 105 °C. After 15 h, small transparent crystals began to appear. After the completion of the experiment after 20–24 h, the crystals were checked by powder XRD, and the diffractogram showed the presence of MOF-5 exclusively.

For the experiments with low initial water content, a water-free solution of zinc nitrate in DEF was prepared by dissolving anhydrous ZnCl<sub>2</sub> (Riedel-de Haen) and AgNO<sub>3</sub> (KMF Laborchemie Handels-GmbH) in dried DEF and filtering off the resulting AgCl precipitate. To avoid any water contamination, the preparation of the reaction solutions and the filling of the autoclave were carried out under argon atmosphere in a glove box. For the isotope experiments, deuterated terephthalic acid (D<sub>2</sub>BDC) was prepared by reacting NaOD in D<sub>2</sub>O (99.2% D, Chemotrade Leipzig) with H<sub>2</sub>BDC. After filtration, the reaction product Na<sub>2</sub>BDC was reacted with DCl in D<sub>2</sub>O (98% D, Chemotrade Leipzig) to precipitate D<sub>2</sub>BDC. The purity of D<sub>2</sub>BDC was checked by the absence of the characteristic broad FTIR ν(O-H)<sup>-</sup> signal in the 2300–3300 cm<sup>-1</sup> range.

## Results

**Chemical Composition of the Gas-Phase.** A typical gas-phase mass spectrum after the completion of a standard MOF-5 synthesis at 24 h is shown in Figure 1. The largest peak at mass 44, besides the peak of the carrier gas argon at mass 40, can be identified by the cracking pattern and by the comparison with the FTIR measurements as being predominantly CO<sub>2</sub>. The FTIR measurements do not show any signs of CO. The CO<sub>2</sub> signal is followed in intensity by the hydrogen one at mass 2. Another species identified via FTIR is N<sub>2</sub>O (signals at 2240 and 2270 cm<sup>-1</sup>), while there is no sign of any other nitrogen oxides, such as NO or NO<sub>2</sub><sup>-</sup>. The differences of the mass signals 44, 28, and 14 as compared to the cracking pattern of CO<sub>2</sub> suggest that there are only small amounts of N<sub>2</sub> (<2%). Traces of water were also detected by QMS. The release of CO<sub>2</sub> in conjunction with the release of N<sub>2</sub>O and N<sub>2</sub> indicates that the oxidative power

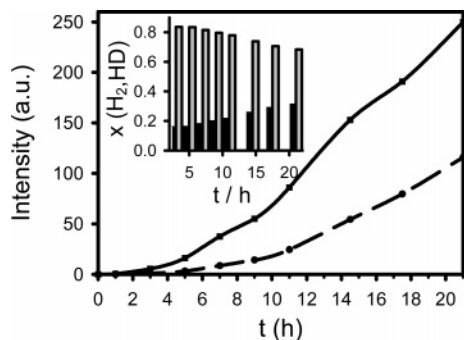
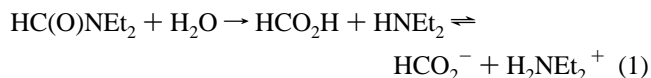
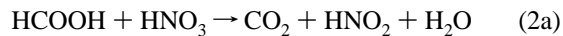


**Figure 2.** Hydrogen evolution during a MOF-5 synthesis from  $\text{Zn}(\text{NO}_3)_2 \cdot 4\text{D}_2\text{O}$  and  $\text{D}_2\text{BDC}$ ; QMS, intensities of mass 2 (dashed line) and mass 3 (solid line). For the first few hours (3–11 h), the total hydrogen release seems to grow exponentially and eventually approaches a nearly linear form. Insert: Contribution of  $\text{H}_2$  (black bars) and  $\text{HD}$  (gray bars) to the total hydrogen signal. The contribution of  $\text{H}_2$  to the total hydrogen signal increases from initially 16 to 32% toward the end of the experiment. This fact can be explained by the assumption that the product water of the reactions 2 and 4 in Scheme 1 contributes to reaction 1. Small contributions of mass 4, reflecting  $\text{D}_2$  (<0.5%), were neglected.

of the nitrate in the presence of  $\text{H}^+$  is responsible for the oxidation of the carbon-containing species. Because of its stability,  $\text{H}_2\text{BDC}$  is less likely to be the carbon source than the solvent, especially since, in the presence of water, DEF will undergo the well-known acid catalyzed hydrolysis reaction:



A quantitative analysis by NMR of how much solvent was hydrolyzed will be given further below. After reaction 1 has occurred, formic acid will react with nitric acid. For this reaction, several reaction pathways are known, creating all together a product spectrum that already accounts for the occurrence of  $\text{CO}_2$ ,  $\text{N}_2\text{O}$ , and  $\text{N}_2$ .



As was tested in a separate experiment,  $\text{HNO}_3$ , DEF, and water at room temperature will strongly react and the reduction of  $\text{HNO}_3$  with formic acid will produce only  $\text{CO}_2$  and  $\text{N}_2$  without the formation of any gaseous nitrogen oxides. It is important to notice that all of these solvent decomposition pathways do not account for the other pronounced feature in the experiment, the evolution of molecular hydrogen (Figure 1).

**Origin of the Gas-Phase Component  $\text{H}_2$ .** As a source of hydrogen in this highly oxidative environment, there are potentially three different types of hydrogen atoms conceivable: protons from carboxylic acid or water, fairly inert hydrogens located at the ethyl groups of the solvent and at the aromatic ring of  $\text{H}_2\text{BDC}$ , and the hydrogen atom at the amide group, hereinafter called formyl hydrogen. To check to which extent the formyl hydrogen takes part in the evolution of molecular hydrogen, hydrogen was replaced by deuterium in the carboxylic group of the terephthalic acid, which was subsequently added together with  $\text{D}_2\text{O}$  to a water-free zinc nitrate DEF solution. The hydrogen evolution over time during a MOF-5 synthesis with deuterated species is shown in Figure 2. Because of the inertness of the ethyl and aromatic hydrogens,

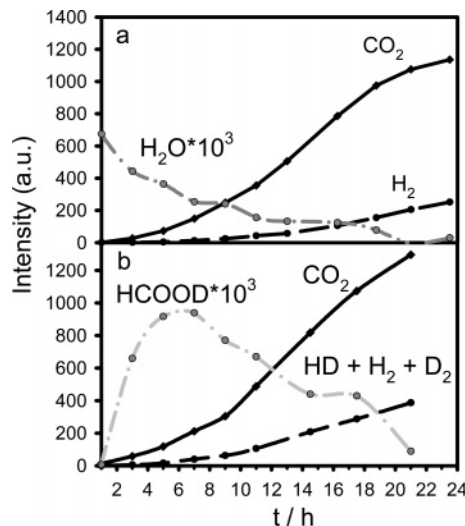


**Figure 3.** Development of the content of  $\text{CO}_2$ ,  $\text{H}_2$ , and  $\text{H}_2\text{O}$  (a) and the content of  $\text{CO}_2$ ,  $\text{HCOOD}$ , and the sum of all hydrogen species (b) in the gas-phase of a solvothermal MOF-5 synthesis. The curves were corrected for the pressure drops occurring when samples were taken.

the primary product  $\text{HD}$  can be seen as a demonstration that the observed evolution of molecular hydrogen requires the decomposition of the solvent molecule. During the hydrolysis of DEF (reaction 1), the formyl hydrogen is not released and remains in the same chemical environment, that is, being afterward located in the formyl group of the product formic acid. Therefore, another reaction step now decomposing the formic acid is needed to release it. Because the oxidation under the reaction conditions of formic acid in DEF by  $\text{HNO}_3$  as aforementioned did not reveal any hydrogen release, another mechanism, from now on called the direct mechanism, needs to be postulated.

Because of the stabilizing effect of a higher proton activity on formic acid and the diethylammonium ion, we tested the decomposition of a solution of formic acid and diethylamine in DEF at 100 °C without any additional proton source ( $\text{H}_2\text{BDC}$ ) and found as reaction products only  $\text{H}_2$  and  $\text{CO}_2$  in equal amounts in the gas phase.



This reaction is related to hydrogenation reactions in organic synthesis using ammonium formate with  $\text{Pd/C}$  as a catalyst for the hydrogen transfer.<sup>30,31</sup> Reaction 3 is also compatible with the observation of  $\text{HD}$  being the primary molecular hydrogen product of the deuterium experiments. Thus, this decomposition pathway can be assumed to be the main source for the hydrogen evolution observed. Because this reaction is essentially the direct decomposition of the thermodynamically unstable formic acid without the involvement of a permanently altered reaction partner (diethylamine can be seen as being only a catalyst), the term direct mechanism for this formic acid decomposition pathway was chosen. It is also noteworthy that for this ion reaction to happen, both reaction partners must not be simultaneously present in their protonated forms. Thus, a high proton activity reduces the contribution of the direct mechanism to the formic acid decomposition.

**Temporal Development of Gaseous Species during a MOF-5 Synthesis.** To address the issue of having potentially multiple  $\text{CO}_2$  sources, we performed quasi *in situ* investigation of the gas-phase composition over time. The results of a deuterated and a nondeuterated experiment are shown in Figure

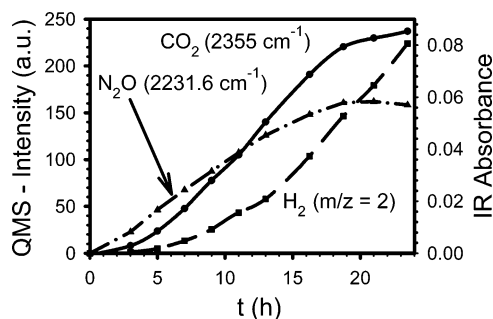


**Figure 4.** Comparison of the temporal development of the  $\text{N}_2\text{O}$ ,  $\text{CO}_2$ , and  $\text{H}_2$  content in the gas-phase during a MOF-5 synthesis. The  $\text{N}_2\text{O}$  and  $\text{CO}_2$  contents were measured by FTIR,  $\text{H}_2$  by mass spectrometry.  $\text{N}_2\text{O}$  was chosen as a tracer molecule of the nitrate reduction processes occurring in the reaction solution. Because the strongest  $\text{CO}_2$  line was close to saturation, a line with lower intensity at 2355  $\text{cm}^{-1}$  was chosen.

3. Displayed is the evolution of  $\text{CO}_2$ ,  $\text{H}_2$ ,  $\text{H}_2\text{O}$ , and  $\text{HCOOD}$ . In Figure 3b, the total hydrogen evolution, that is, the sum of  $\text{H}_2$ ,  $\text{D}_2$ , and  $\text{HD}$ , is shown. As can be seen in the deuterium isotope experiments in Figure 1b, a new peak at mass 47 appears that corresponds to the deuterated formic acid formed by the hydrolysis reaction 1. We therefore track formic acid by mass 47 in isotope experiments (Figure 3b). At the beginning, the evolution of  $\text{CO}_2$  and, with some delay, the one of hydrogen (Figure 3a) too, both show an exponential-like increase. The production rate of hydrogen, that is, the slope of the corresponding curve, becomes approximately constant toward the end of the experiment. While the hydrogen production reaches its maximum there, the  $\text{CO}_2$  rate has already declined, noticeable in the turning point at around  $t = 16$  h. After this point, the rate falls back to a lower level. Because of the long duration of the experiment, it is not clear if an approximately constant level can eventually be reached. Calculating the final  $\text{CO}_2$  as well as the final hydrogen production rate for the standard experiment shown in Figure 3a, a ratio of approximately 1:0.77 is reached. Everywhere else, the  $\text{CO}_2$  production rate exceeds the hydrogen one by a larger factor. The constant  $\text{CO}_2$  production rate toward the end of the experiment is confirmed by the gas-phase FTIR measurements of another standard MOF-5 experiment shown in Figure 4. These measurements also show that in contrast to the content of  $\text{CO}_2$  and  $\text{H}_2$ , the one of  $\text{N}_2\text{O}$ , as a representative species of the nitrate reduction pathways, saturates in the gas-phase. The content of formic acid goes through a maximum as can be seen in Figure 3b. If one assumes that the gas-phase concentration is almost in equilibrium with the formic acid concentration in the solution, the curve indicates that a significant change in the formic acid production and decomposition rate occurs.

Because some of the decomposition pathways, that is, the subsequent reaction of 1 and 2c or of 1 and 2a and 4, are related to water production, we also used the gas-phase water concentration as a tracer to obtain information about the water content in the solution. In a successful MOF-5 synthesis, the water content declines rapidly as can be seen in Figure 5. From the fact that the formic acid concentration goes through a maximum and the observation that there was no crystal formation visible by the eye, if the experiment was performed in closed glass vessels, before this maximum was passed, one can conclude that the reaction needs first to alter the conditions where MOF-5 can be formed and is stable. If this is correct, it is conceivable that small parameter changes that are able to alter the balance of the reactions kinetics of the individual reaction steps may have a large influence on the final product. This fits to our

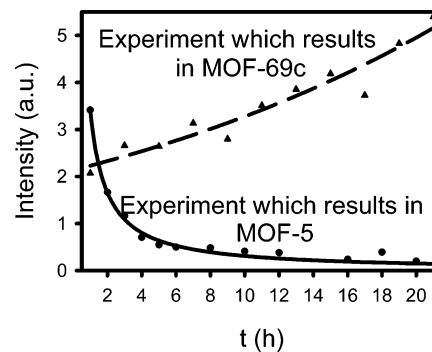


**Figure 5.** Intensity of mass 18 in the gas-phase of two different experiments using the same chemical composition of the initial reaction solution. Circles: A glass insert for the autoclave was used. In this experiment, the water content decreased and MOF-5 was obtained exclusively. Triangles: A PTFE insert was used. The water content in the gas-phase increased over time, and the final product was primarily MOF-69c. The lines are guided by the eye.

**TABLE 1: Reactants and Products Contents before and after a MOF-5 Synthesis (Species in Solution in mmol)**

	start	end	diff.	diff. %
$\text{Zn}^{2+}\text{a}$	4.2	2.37	1.83	43.6
$\text{NO}_3^-\text{b}$	8.4	5.67	2.73	32.5
water <sup>c</sup>	16.8	10.0	6.8	40.5
$\text{HNEt}_2\text{d}$	0	$4.2 \pm 0.2$		
$\text{Et}_2\text{NNO}\text{d}$	0	$2.8 \pm 0.5$		
$\text{H}_2:\text{CO}_2\text{e}$	0	1:2.4		

<sup>a</sup>  $\text{Zn}^{2+}$  content measured by ICP-OES. <sup>b</sup>  $\text{NO}_3^-$  content measured by ion chromatography. <sup>c</sup> Amount of water measured by Karl Fischer titration. <sup>d</sup>  $^{13}\text{C}$  inverse-gated proton-decoupled NMR. The values given are the average of all available signals for that species. Errors are given by the maximal deviation of a signal from the average. <sup>e</sup>  $\text{CO}_2$  content expressed as a multiple of the hydrogen partial pressure.

observation that although MOF-5 could be reliably generated in autoclave glass inserts, in PTFE liners sometimes MOF-69c is generated. To see how such a reaction process deviates from a successful MOF-5 experiment, we tracked its gas-phase water content over time. The result is displayed in Figure 5. The powder XRD diffractogram of the synthesis shows only the presence of MOF-69c with no traces of MOF-5. The evolution of  $\text{H}_2$  and  $\text{CO}_2$  (not shown here) is qualitatively the same as in the MOF-5 syntheses. The water curve, however, displays the opposite behavior, that is, a strong increase of the water content as compared to the MOF-5 case. It is clear that only the zinc hydroxide carboxylate MOF (MOF-69c) as compared to the zinc oxide carboxylate MOF (MOF-5) can coexist with a high water content in the reaction solution, since the oxide ion will not be able to survive the water attack.

**Reactants and Byproducts in the Liquid-Phase.** To understand the basic reaction scheme and especially the aspects of the proton and water management in the MOF-5 synthesis, it is necessary to identify and quantitatively determine the changes of the concentrations of the most relevant species. We therefore measured their amounts in the reaction solution at the beginning and after the synthesis. The results are listed in Table 1.

The diethylammonium/diethylamine concentrations were determined by  $^{13}\text{C}$  NMR and  $^1\text{H}$  NMR. Because of the fast proton exchange, the NMR measurement does not clearly distinguish between these two species. The species were identified by the 3.05, 1.37 ppm ( $^1\text{H}$  NMR) and 42.49, 11.29 ppm ( $^{13}\text{C}$  NMR) signals in comparison with ref 32. In addition to the species discussed so far, the compound N-nitrosodiethyl-

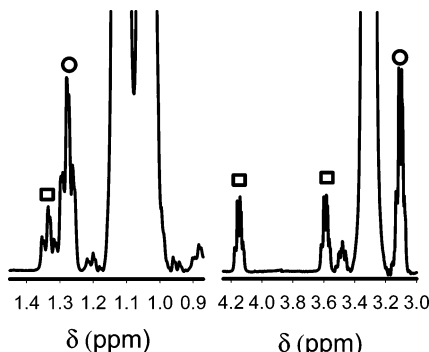


**Figure 6.** Methyl (left) and methylene region (right) in the  $^1\text{H}$  NMR spectra of the reaction solution after the completion of a standard MOF-5 experiment. The signals marked by a circle belong to  $\text{HNEt}_2$  in free, protonated, and coordinated form. The signals marked by a square belong to N-nitrosodiethylamine. The broad absised signals belong to the solvent DEF.

amine was identified by the  $^1\text{H}$  and  $^{13}\text{C}$  NMR measurements in comparison with ref 33 and a 0.3 M reference solution of  $\text{Et}_2\text{NNO}$  (Sigma-Aldrich, 99%) in DEF. The corresponding peak positions are at 3.59, 4.15, and 1.37 ppm and 37.9, 11.0, 46.6, and 14.0 ppm, respectively. Pure  $\text{Et}_2\text{NNO}$  displays four  $^1\text{H}$  signals, but one is superimposed with a DEF signal and was not used here. Despite the similarity of the structures, the peak separation allows the clear distinction between the various amine-based reaction products as can be seen in the  $^1\text{H}$  NMR shown in Figure 6.

Because there is almost no peak overlap in the decoupled  $^{13}\text{C}$  NMR measurements, we used these signals for the quantitative determination of amine and N-nitrosodiethylamine concentrations. The solvent signal was used as an internal standard. The spectra were taken using inverse-gated proton decoupling, a 30° flip angle, and an averaging of 744 scans with a scanning rate of 20 s/scan. The results were confirmed by the corresponding  $^1\text{H}$  NMR analysis. Because N-nitrosodiethylamine

must result from the nitrate decomposition, it is of interest to compare its amount to the total nitrate loss. As can be seen from Table 1, the total nitrate loss during the MOF-5 synthesis is almost identical with the amount of N-nitrosodiethylamine formed. This observation fits to the fact that only a fairly small amount of nitrogen-containing species can be found in the gas-phase. Thus, one can conclude that most of the nitrogen resulting from the nitrate decomposition will ultimately stay in the liquid-phase and be bound by amine. It also means that out of the reactions Scheme 2a–c, 2a is most likely the dominating one, since  $\text{HNO}_2$  is well-known to react with amines to N-nitrosoamines according to

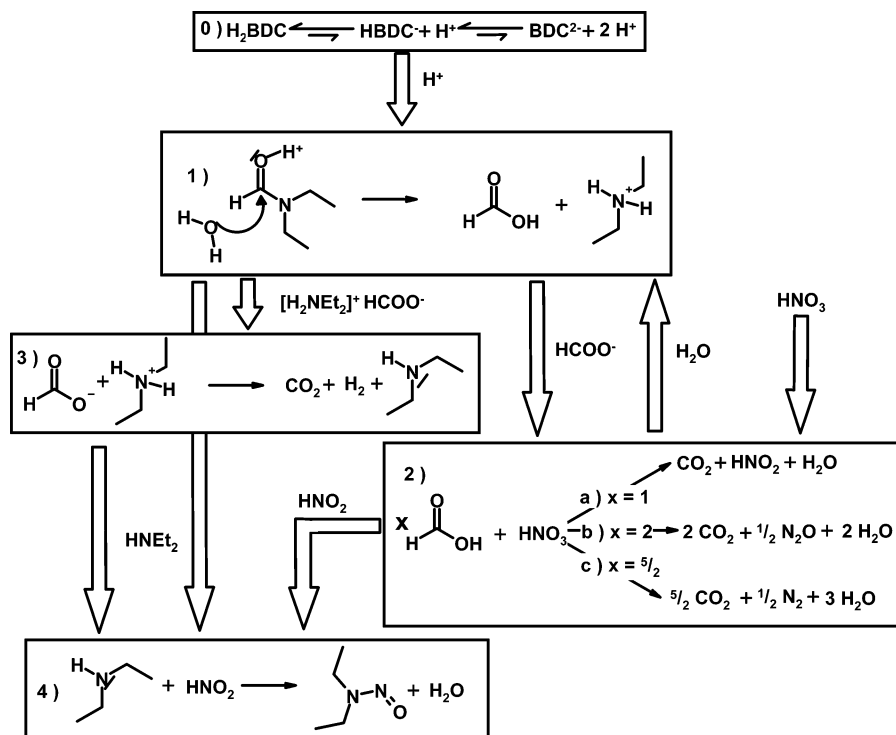


The most striking result taken from Table 1 is the reduction of the water content during the 24 h reaction time. The final concentration is only two-thirds of its initial value. At the same time, the relatively high concentration of all amine products allows us to estimate how much solvent was hydrolyzed (see Discussion). The loss of nitrate is relatively low and also does not match the production of all amine type reaction products.

## Discussion

**Quantitative Contributions of Different Reaction Pathways.** Scheme 1 summarizes the results and conclusions of the experiments presented so far. If we assume that this reaction scheme is already a good representation of the whole process, we can estimate the contributions of the different reaction pathways from the ratio of the partial pressures of the two gaseous products  $\text{H}_2$  and  $\text{CO}_2$  in combination with the products in the reaction solution. The ratio of the  $\text{H}_2$  to  $\text{CO}_2$  partial pressures was determined as 1:2.4 (Table 1). Although this result was achieved by the use of a mass spectrometer calibrated with hydrogen carbon dioxide mixtures, it essentially agrees with the ratio of the corresponding peak intensities shown in Figure

### SCHEME 1: Postulated Reaction Pathways for the Solvothermal MOF-5/MOF-69c Synthesis Based on Zinc Nitrate and $\text{H}_2\text{BDC}$ in DEF



1. As was concluded earlier from the nitrate loss vs the Et<sub>2</sub>NNO production, the dominant nitrate decomposition reaction is reaction 2a. Because this reaction releases one molecule of CO<sub>2</sub> per one molecule of formate, as does the hydrogen-producing reaction, the ratio of the contributions of reactions 3 and 2a to the formate decomposition is 1:1.4, respectively. These data clearly indicate that the role of the direct mechanism goes beyond a simple side reaction but is probably a fundamental element of the MOF-5 synthesis.

Further analysis can be based on the species in solution that show little volatility. These species are nitrate, Zn<sup>2+</sup>, and the amine species, that is, HNEt<sub>2</sub> and Et<sub>2</sub>NNO. HNEt<sub>2</sub> and Et<sub>2</sub>NNO are not considered as being volatile since they were not found in the QMS measurements. Assuming that all amine-based reaction products were created by the hydrolysis reaction 1, as well as assuming that there is no pathway for the decomposition of any amine-based reaction products, a total decomposition of 7.0 ± 0.7 mmol solvent molecules (ca. 7%) took place. This in turn should have led to the formation of the same amount of formate. The nitrate loss of 2.73 mmol, which is approximately the amount of Et<sub>2</sub>NNO formed, is a direct measure for the formate decomposition by the nitrate pathway 2. According to the hydrogen to CO<sub>2</sub> ratio, the direct mechanism should then have led to a decomposition of 1.95 mmol of formate. As was shown by this analysis, the direct mechanism is quantitatively comparable to the one involving the nitrate reduction via HNO<sub>3</sub> (nitrate mechanism), but most likely, it is of particular importance because it is so far the only reaction that eliminates formate/formic acid without producing water.

**Water Balance and Proton Activity.** Immersing small amounts of MOF-5 in a solution of Zn(NO<sub>3</sub>)<sub>2</sub>·4H<sub>2</sub>O in DEF (0.18 M), with so much water added that the total water concentration reaches 1.13 M, results, at 100 °C, in the complete conversion of MOF-5 to MOF-69c within 4 h. The given water and zinc nitrate concentrations approximately reflect the reaction conditions that would exist at the end of the standard experiment if all hydrate water that corresponds to the amount of zinc that went into the MOF-5 formation were released into the reaction solution and if there were no water-removing reaction steps present. The value 1.13 M also takes into account that one water molecule per four zinc atoms may be needed for the creation of the oxide ion. The observed structural conversion is a strong indicator that water removal is a prerequisite for a successful MOF-5 synthesis. At first sight, one would attribute the water removal to the hydrolysis reaction, but as will be discussed below, the hydrolysis can only be effective if there is no or little water production by the subsequent reactions involving the hydrolysis products. Even if the final water content were too high for the existence of MOF-5, the initial water activity could still be low enough due to its coordination to the metal center to allow the formation of MOF-5 directly at the beginning of the experiment. If the water were sufficiently bonded to the metal center, its partial pressure would have to be comparably low. We therefore compared the mass 18 signal of the gas-phase of the standard experiment prepared with Zn(NO<sub>3</sub>)<sub>2</sub>·4H<sub>2</sub>O with the one of a DEF solution containing the same amount of water and found that in the presence of zinc nitrate the partial pressure is lowered only by approximately 20%. This comparably small change can be seen as a clear sign that the initial water activity is high and must still be lowered as a prerequisite for the MOF-5 formation to start.

Concerning the proton activity, it is either too high for the survival of an oxide ion and the doubly deprotonated terephthalic acid, that is, for the existence of MOF-5, right at the beginning

of the experiment, or would become too high during the course of the reaction due to the removal of BDC<sup>2-</sup> if there were no proton-removing reaction steps. The latter possibility, however, does not fit to the observation that MOF-5 forms only after an induction period of several hours. It is therefore reasonable to assume that the induction period corresponds to the lowering of the water and proton activities during the reaction's progress.

The proton activity can be lowered via the acid-catalyzed hydrolysis of the solvent in two ways (box 1, Scheme 1): First, by the provision of a base, that is, diethylamine, which is more strongly basic than the solvent itself; second, by the removal of the hydrolysis product formic acid by redox reactions transforming it into products, most of them gaseous, that are mainly removed from the reaction solution. The latter process can be also carried out in two different ways leading to different sets of gaseous products. The oxidation can be either due to the presence of HNO<sub>3</sub> or due to the direct mechanism. The oxidation by nitric acid can theoretically happen according to the reactions 2a–c (Scheme 1), but because the amount of Et<sub>2</sub>NNO almost matches the amount of nitrate lost and because there were almost no gaseous reaction products of the reactions 2b and 2c found in the gas-phase, we conclude that 2a dominates by far. Because this oxidation step dominates and produces in connection with reaction 4 more water than was consumed during the production of the corresponding amount of formic acid by the hydrolysis reaction, the nitrate mechanism leads to a net water production. As a consequence of the formic acid decomposition by this route, the destructive proton activity is lowered, but at the same time, the also undesired water content will go up. Only the formic acid decomposition reaction pathway via reaction 2b in connection with reaction 1 is water neutral. Because a total net reduction of the water content was found experimentally, the rate of the water-removing hydrolysis reaction must quantitatively exceed all water-producing reactions rates. Experimental evidence for the water reduction can be directly seen in Table 1 or in Figure 5.

The final water content in the solution is then determined by the water content at the beginning of the experiment, the amount used for the hydrolysis reaction, potentially by the amount used for the creation of the oxide ion, and the amount of water that is produced by the nitrate mechanism. The minimal amount of water that was removed by the hydrolysis reaction is given by the sum of the amine species (7 mmol). Even if it is assumed that the oxide is formed from water exclusively, its maximal contribution to the overall water loss would be comparably small (0.46 mmol, i.e., a quarter of the Zn<sup>2+</sup> loss). On the basis of the conclusion that almost all nitrate reacts according to 2a and 4, thereby producing two molecules of water per nitrate molecule, a water production of 5.46 mmol is calculated. From these contributions, the final water content should be 14.8 mmol instead of the measured 10.0 mmol. The difference raises the question if there are other water-reducing processes, but so far, the best explanation is given by water removal by the precipitated MOF product, small losses by evaporation, and some experimental error.

Because both formic acid decomposition routes, the nitrate and the direct one, do lower the proton activity, one can ask how these contributions change with the reaction's progress. According to Figure 3, the hydrogen evolution rate as the main characteristic of the direct mechanism is initially low in relation to the CO<sub>2</sub> production rate and then continuously increases with the reaction's progress. This observation fits well to the conclusion following the introduction of reaction 3 that a high proton activity should inhibit the direct mechanism. To test the

assumption further if a lower proton activity benefits the direct mechanism in relation to the nitrate one, we performed the standard MOF-5 experiment without terephthalic acid and also found, similarly to reaction 3, only H<sub>2</sub> and CO<sub>2</sub> in equimolar amounts in the gas-phase and ZnO as a solid reaction product. Essentially no nitrogen-containing reaction products were found in the gas-phase.

Although according to Figure 3 the direct mechanism may eventually prevail, the nitrate one definitely dominates at the beginning. Because the initial proton activity can be assumed to be high, the nitrate mechanism, which needs HNO<sub>3</sub>, not nitrate, as the oxidizing agent must lose its strength with decreasing proton activity and should therefore have its strongest influence at the beginning. An experimental indicator for the decrease of the efficiency of the nitrate mechanism vs the direct mechanism can be seen by the saturation of the N<sub>2</sub>O curve toward the end of the experiment in Figure 4, whereas the CO<sub>2</sub> and hydrogen content still increases almost linearly as predicted by reaction 3. Although, as was concluded earlier from QMS measurements, the ratio of the CO<sub>2</sub> to H<sub>2</sub> with 1:0.77 rate has not yet fully reached parity.

The total CO<sub>2</sub> production is governed by the individual rates of the hydrolysis reaction and the two subsequent parallel reactions, the direct and the nitrate one. Additional information about the relationship between these different rates may come from the temporal formic acid/formate development. The asymmetric shape of the HCOOD curve in Figure 3b indicates that at the beginning the formic acid net production rate must be significantly faster than the decomposition reaction rates. Although it is not clear at this point what changes in the reaction conditions cause the decomposition rate to win over the production kinetics, there are two general possibilities: First, by a decline of the formic acid/formate production rate, either by the reduction of the water content or, because the hydrolysis reaction is known to be acid-catalyzed, by the reduction of the proton activity, and second, by an increase of the formic acid/formate decomposition rate by switching from the nitrate mechanism to the direct one. The latter would be another consequence of the decline of the proton activity during the reaction. As an indication for the involvement of the direct mechanism in this process, it is important to notice that the formic acid build-up clearly predates the hydrogen release.

## Summary and Conclusion

From gas-phase investigations of the widely used synthesis of MOF-5 in DEF, we identified an unexpected solvent decomposition pathway that is capable of lowering the proton activity as well as supporting the removal of water from the reaction solution. Both properties are essential for the stabilization of the oxide ion in MOF-5 by the reaction. The best evidence for this pathway is the release of molecular hydrogen. Isotope experiments demonstrated that the hydrogen release involves the formyl hydrogen of the solvent and cannot be explained simply by heterolytic splitting of the water during the oxide formation. The solvent decomposition produces diethylamine as a base and formic acid/formate. By means of the analysis of the gaseous reaction byproducts in combination with the quantitative determination of the main liquid-phase reaction products, the irreversible removal of formic acid from the solution, thereby lowering the proton activity, was demonstrated. Temporal records of the production rate of the gaseous species suggest that along with the change of the proton activity the solvent decomposition switches from nitrate reduction-based pathways to the newly identified one. Although hydrolysis

the main reaction to remove water from the solution, subsequent reaction steps can compensate this effect, thus possibly giving the newly identified reaction step the key role in the water management to arrive at concentrations that allow the formation of zinc oxide carboxylate-based MOFs.

As long as the carboxylate-based linkers do not carry special functional groups that may interfere with the creation of the network formation, the results can be generalized to the whole class of zinc oxide carboxylate-based MOFs. The result is valuable for the design of new oxide-based MOFs applying similar synthesis routes. A quantitative study of the exact water influence on the formation of MOF-5 vs MOF-69c would be of great value.

**Acknowledgment.** We thank Edwin Weber for helping with the financial support for S.H. We thank Beate Kutzner, Anke Schwarzer, and Jörg Wagler for their collaboration in some experiments.

## References and Notes

- (1) Eddaoudi, M.; Kim, J.; Rosi, N. L.; Vodak, D. T.; Wachter, J.; O'Keeffe, M.; Yaghi, O. M. *Science* **2002**, 295, 469.
- (2) Chae, H. K.; Siberio-Pérez, D. Y.; Kim, J.; Go, Y.-B.; Eddaoudi, M.; Matzger, A. J.; O'Keeffe, M.; Yaghi, O. M. *Nature* **2004**, 427, 523.
- (3) Rowsell, J. L. C.; Millward, A. R.; Park, K. S.; Yaghi, O. M. *J. Am. Chem. Soc.* **2004**, 126, 5666.
- (4) Wong-Foy, A. G.; Matzger, A. J.; Yaghi, O. M. *J. Am. Chem. Soc.* **2006**, 128, 3494.
- (5) Millward, A. R.; Yaghi, O. M. *J. Am. Chem. Soc.* **2005**, 127, 17998.
- (6) Panella, B.; Hirscher, M. *Adv. Mater.* **2005**, 17, 538.
- (7) Dailly, A.; Vajo, J. J.; Ahn, C. C. *J. Phys. Chem. B* **2006**, 110, 1099.
- (8) Li, Y. *J. Am. Chem. Soc.* **2006**, 128, 726.
- (9) Stallmach, F.; Gröger, S.; Küntzel, V.; Kärger, J.; Yaghi, O. M.; Hesse, M.; Müller, U. *Angew. Chem., Int. Ed.* **2006**, 45, 2123.
- (10) Chen, B.; Liang, C.; Yang, J.; Contreras, D. S.; Clancy, Y. L.; Lobkovsky, E. B.; Yaghi, O. M.; Dai, S. *Angew. Chem., Int. Ed.* **2006**, 45, 1390.
- (11) Hermes, S.; Schröter, M.-K.; Schmid, R.; Khodeir, L.; Muhler, M.; Tissler, A.; Fischer, R. W.; Fischer, R. A. *Angew. Chem., Int. Ed.* **2005**, 44, 6237.
- (12) Hermes, S.; Schröder, F.; Chelmowski, R.; Wöll, C.; Fischer, R. A. *J. Am. Chem. Soc.* **2005**, 127, 13744.
- (13) Li, H.; Eddaoudi, M.; O'Keeffe, M.; Yaghi, O. M. *Nature* **1999**, 402, 276.
- (14) Choi, J. Y.; Kim, J.; Jhung, S. H.; Kim, H.-K.; Chang, J.-S.; Chae, H. K. *Bull. Korean Chem. Soc.* **2006**, 27, 1523.
- (15) Mueller, U.; Schubert, M.; Teich, F.; Puettner, H.; Schierle-Arndt, K.; Pastre, J. *J. Mater. Chem.* **2006**, 16, 626.
- (16) Yaghi, O. M.; O'Keeffe, M.; Ockwig, N. W.; Chae, H. K.; Eddaoudi, M.; Kim, J. *Nature* **2004**, 423, 705.
- (17) Ferey, G.; Mellot-Draznieks, C.; Serre, C.; Millange, F.; Dutour, J.; Surble, S.; Margiolaki, I. *Science* **2005**, 309, 2040.
- (18) Sabo, M.; Boehlmann, W.; Kaskel, S. *J. Mater. Chem.* **2006**, 16, 2354.
- (19) Edgar, M.; Mitchell, R.; Slawin, A. M. Z.; Lightfoot, P.; Wright, P. A. *Chem. Eur. J.* **2001**, 7, 5168.
- (20) Clausen, H. F.; Poulsen, R. D.; Bond, A. D.; Chevallier, M.-A. S.; Iversen, B. B. *J. Solid State Chem.* **2005**, 178, 3342.
- (21) Liao, J. H.; Lee, T. J.; Su, C. T. *Inorg. Chem. Commun.* **2006**, 9, 201.
- (22) Sun, J.; Zhou, Y.; Fang, Q.; Chen, Z.; Weng, L.; Zhu, G. *Inorg. Chem.* **2006**, 45, 8677.
- (23) Rowsell, J. L. C.; Yaghi, O. M. *J. Am. Chem. Soc.* **2006**, 128, 1304.
- (24) Loiseau, T.; Muguerra, H.; Ferey, G.; Haouas, M.; Taulelle, F. *J. Solid State Chem.* **2005**, 178.
- (25) Burrows, A. D.; Cassar, K.; Friend, R. M. W.; Mahon, M. F.; Rigby, S. P.; Warren, J. E. *CrystEngComm* **2005**, 7, 548.
- (26) Rosi, N. L.; Kim, J.; Eddaoudi, M.; Chen, B.; O'Keeffe, M.; Yaghi, O. M. *J. Am. Chem. Soc.* **2005**, 127, 1504.
- (27) Greathouse, J. A.; Allendorf, M. D. *J. Am. Chem. Soc.* **2006**, 128, 10678.

- (28) Rowsell, J. L. C.; Yaghi, O. M. *Microporous Mesoporous Mater.* **2004**, *73*, 3.
- (29) Biemmi, E.; Bein, T.; Stock, N. *Solid State Sci.* **2006**, *8*, 363.
- (30) Johnstone, R. A. W.; Wilby, A. H.; Entwistle, I. D. *Chem. Rev.* **1985**, *85*, 129.
- (31) Ram, S. W.; Ehrenkaufer, R. E. *Synthesis* **1988**, *91*.
- (32) Pouchert, C. J.; Behnke, J. *The Aldrich Library of <sup>13</sup>C and <sup>1</sup>H NMR Spectra*, 1st ed.; Aldrich Chemical Co.: Milwaukee, WI, 1993; Vol. 1, p 472.
- (33) (a) Pregosin, P. S.; Randall, E. W. *Chem. Commun.* **1971**, 399. (b) Looney, C. E.; Phillips, W. D.; Reilly, E. L. *J. Am. Chem. Soc.* **1957**, *79*, 6136.